Pertanika J. Sci. & Technol. 33 (2): 1007 - 1030 (2025)

PERTANIKA JOURNALS

SCIENCE & TECHNOLOGY

Journal homepage: http://www.pertanika.upm.edu.my/

Hydrogenolysis of Glycerol to Propanediols over Ni supported on MgO Catalyst

Maryam Shakur*, Maryum Irshad and Muhammad Sajjad Haider

Department of Chemical Engineering, University of Engineering & Technology, Lahore 54890, Pakistan

ABSTRACT

A Ni/MgO catalyst was used to undergo hydrogenolysis of glycerol, a byproduct of biodiesel synthesis, in the aqueous phase at different nickel loadings (10–40% by weight). The wet impregnation-prepared catalysts were characterized by XRD, SEM, TPR, and BET methods and showed strong metal-support interaction, good Ni dispersion, and high surface area, respectively. The catalytic activity in a batch reactor was measured at 220°C, 3 MPa hydrogen pressure, and 20 hours of reaction time. Glycerol conversion exhibited an increasing trend with Ni loading in the following sequence: 10%Ni/MgO < 20%Ni/MgO < 30%Ni/MgO < 40%Ni/MgO. The 20%Ni/MgO catalyst yielded the highest 1,2-propanediol (1,2-PDO) production, with a subsequent decrease observed at higher Ni loadings. In particular, the 20%Ni/MgO catalyst produced a 74% total glycerol conversion and a 76% selectivity toward 1,2-PDO. The optimal reaction conditions were then ascertained by examining the effects of temperature (200–240°C), glycerol content (5%–30% by weight), hydrogen pressure (3–5 MPa), and reaction time (6–25 hours) on the activity of the 20%Ni/MgO catalyst.

Keywords: Biomass; catalysis; glycerol; green economy; hydrogenolysis; Ni/MgO

INTRODUCTION

Prices have increased, and carbon emissions have increased because of the growing demand for and decreased availability of fossil fuels. Biofuel production offers a crucial alternative to meet energy needs and reduce the carbon footprint (Quispe et al., 2013). Biodiesel, a sustainable fossil fuel alternative, produces significant glycerol byproducts (Gonzalez-Garay et al., 2017). Increasing biodiesel production has boosted

ARTICLE INFO

Article history:
Received: 13 September 2024
Accepted: 16 January 2025
Published: 07 March 2025

DOI: https://doi.org/10.47836/pjst.33.2.21

E-mail addresses:
maryamshakur@hotmail.com (Maryam Shakur)
irshadmm@mail.uc.edu (Maryum Irshad)
sajjadhaider51272@gmail.com (Muhammad Sajjad Haider)
*Corresponding author

ISSN: 0128-7680
e-ISSN: 2231-8526

glycerol supply, posing challenges. Converting excess glycerol into valuable chemicals like propanediols and acrolein can improve biodiesel economics (Sun et al., 2016).

Glycerol hydrogenolysis via catalysis can be directed towards the yield of several alcohols, among which the two most relevant are 1,2-propanediol (1,2-PDO) and 1,3-propanediol (1,3-PDO). 1,2-Propanediol finds usage in the medicine and tobacco sectors. Other important areas for its use are in the manufacture of antifreeze additives, paints, cosmetics and polymers (Bagheri et al., 2015; Nakagawa & Tomishige, 2011). Historically, a petrochemical method that involved the hydration of propylene oxide and hydroperoxide made from propylene or chlorohydrin obtained from oil has been used to create 1,2-PDO (Tendam & Hanefeld, 2011). However, these procedures are both environmentally detrimental and costly (Kumar et al., 2020).

Glycerol hydrogenolysis, in which hydrogen cleaves the C–C and C–O bonds in glycerol, provides a more economical as well as ecologically sound way to produce 1,2-PDO. Along with lower amounts of alcohols, including methanol, ethanol, and ethylene glycol, the process yields a variety of compounds, such as 1,2-propanediol, 1,3-propanediol, acetol, 1-propanol, and 2-propanol (Wang et al., 2019). The catalyst's nature, metal-support interaction, and particle size significantly influence the reaction mechanism and product selectivity. Glycerol hydrogenolysis is generally understood to occur in two steps: Glycerol is hydrogenated after dehydration to create an intermediate to the final product (Vasiliadou & Lemonidou, 2015).

Numerous heterogeneous catalysts have been investigated for glycerol hydrogenolysis. These include those based on noble metals like Pt (Dolsiririttigul et al., 2023), W (Numpilai et al., 2021), Pd and Ru (Salgado et al., 2021), Rh (Wang et al., 2013), Ag (Rekha et al., 2017), and Au (Checa et al., 2012), as well as those based on transition metals like Ni (Azri et al., 2021) Cu (Raju et al., 2020; Wu et al., 2021; Xia et al.,, 2012; Zhou et al., 2010) and Co (Cai, Song et al., 2018). Wang et al. (2013) investigated a range of metal nanoparticles, about 2 nm in size, supported on m-ZrO_2 for the hydrogenolysis of glycerol, including Ru, Rh, Pt, and Pd. The findings showed that the turnover rates were Ru > Rh > Pt > Pd in that order. On the other hand, Pd > Pt > Rh > Ru was the sequence in which the selectivity ratio for the cleavage of C–O to C–C bonds dropped.

Noble metals are too costly for the industrial manufacture of 1,2-PDO despite being efficient and selective in the manufacture of propanediol. The development of catalysts based on first-row transition metals, which are significantly less expensive than second— and third-row noble metals, is advantageous for improving the economic viability of glycerol hydrogenolysis.

Several elements from the d-block, such as Cu, Ni, Co, and Zn, have been studied by researchers as possible catalysts for glycerol hydrogenolysis. Cu-dolomite catalyst has been shown to be effective by Azri et al. (2020), who achieved total glycerol conversion with

92.2% selectivity toward 1,2-PDO at low temperature and pressure. Strong acid sites and low-temperature reduction were identified as critical factors influencing the reaction. The catalyst was stable after five successive reaction cycles, exhibiting 95% conversion and 84% selectivity towards 1,2-PDO. The good activity and selectivity of Cu nanoparticles based on ZnO against propylene glycol was shown by Wang and Liu (2014). Propylene glycol was shown to be produced as a result of the interaction between the metal and support. On the zinc oxide surface, glycerol first experienced dehydration, which produced acetol. Acetol was then hydrogenated on the Cu sites, resulting in the creation of 1,2-PDO. Conversely, when Cu was supported on a basic material such as MgO, the reaction mechanism was altered (Balaraju et al., 2012)

Ni is widely used in industrial catalytic processes, including steam reforming of methane (Rogers et al., 2016; Ross et al., 1978), methane decomposition (Rivas et al., 2008) and glycerol reforming (Seretis & Tsiakaras, 2016). Ni is a good contender for the creation of a less expensive catalyst than Pd- and Pt-based ones since it shares a group in the periodic table with Pd and Pt and frequently displays similar chemistry. Glycerol hydrogenolysis has been thoroughly researched using Ni-based catalysts. Van Ryneveld et al. (2011) evaluated the Ni catalyst's performance in a fixed-bed reactor running at 4 and 7.5 MPa pressures and temperatures between 230 and 320°C. Silica and alumina served as the catalysts' supports. Ni/SiO_2 achieved a glycerol conversion of 99%, while Ni/Al_2O_3 reached 96%. Higher density of active Ni sites and improved reducibility from weaker metal–support interactions were the causes of Ni/SiO_2's superior conversion. However, Ni/Al_2O_3 showed higher selectivity (80%) toward 1,2-PDO in contrast with Ni/SiO_2 (71%) due to the alumina surface's higher concentration of sites containing strong acids.

Reaction activity and selectivity toward 1,2-PDO are improved when the catalyst surface has adequate basic and/or acidic sites (Vasiliadou & Lemonidou, 2015). Mg, Al, Zn, and silica were added to a Ni catalyst supported on CeO_2 to maximize its selectivity toward 1,2-PDO and ethanol. The selectivity toward 1,2-PDO and ethanol was 68% and 9%, respectively, after Mg was added as a promoter on Ni/CeO_2. This work sheds important light on the effects of attaching a basic promoter to an amphoteric support. The addition of zinc and magnesium increased the number of basic sites, increasing the hydrogenolysis activity in terms of conversion and selectivity, according to the study's findings. Menchavez et al. (2017) suggest that the selectivity of the final product is largely dependent on the basicity of the catalyst.

The utilization of monometallic Ni catalysts for glycerol hydrogenolysis has primarily focused on acidic and amphoteric supports, with comparatively limited research available on monometallic Ni catalysts supported on basic materials. Nonetheless, studies on sorbitol hydrogenolysis have looked at the use of Ni/MgO catalysts, showing that, when the same conditions are met, these catalysts have better activity and selectivity than Cu/MgO and

Co/MgO catalysts. Ni/MgO demonstrated a liquid-phase carbon recovery of 91%, sorbitol conversion of 57%, and 33.5% selectivity toward 1,2-PDO at 473 K and 6 MPa of hydrogen pressure. In contrast, when Raney Ni was tested without support under the same operating conditions, both the activity and selectivity toward propanediols were notably lower, highlighting the synergistic role of Ni in conjunction with the MgO support in reaching a high level of selectivity and conversion. Notably, the Raney Ni catalyst also led to a notable rise in the production of gaseous byproducts, suggesting deep hydrogenolysis (X. Wang et al., 2015). In another study investigating sorbitol hydrogenolysis over Ni/MgO, Chen et al. (2013) demonstrated that harsher reaction conditions led to deep degradation and produced more byproducts but increased the overall sorbitol conversion.

The synthesis, characteristics, and catalytic efficiency of many Ni/MgO catalysts with varying Ni loadings are covered in this work. The wet impregnation method was used to manufacture the catalysts and determine how the morphology of the catalysts affected their catalytic performance. XRD, SEM, TPR, and BET tests were used to evaluate them. 20%Ni/MgO catalyst produced the best yield of 1,2-PDO, according to preliminary studies done at a fixed temperature, hydrogen pressure, glycerol feed concentration, and reaction duration. Next, to ascertain the ideal reaction conditions for the chosen 20%Ni/MgO catalyst, a thorough investigation was conducted into the effects of the temperature, hydrogen pressure, fed concentration of glycerol, and reaction time.

MATERIALS AND METHODS

Materials

Nickel nitrate hexahydrate (>98%) was purchased from BDH Chemicals, UK. Glycerol (>99.9%), ethylene glycol (>99.9%), and 1,2-PDO (>99%) were purchased from Fisher Scientific, USA. Methanol (>99.8%), 1-propanol (>99.5%), and 2-propanol (>99.5%) were purchased from Sigma-Aldrich, USA. Merck in Germany was the supplier of ethanol (>99%). Daejung Chemicals, located in South Korea, provided 1-butanol (>99%) and 1,3-PDO (>99%). Acetonitrile (>99.9%) was purchased from Honeywell, USA. Acetol (95%) was purchased from Alfa Aesar, USA. Nitrogen (99.999%) and hydrogen (99.999%) cylinders were purchased from Fine Gas Company, Pakistan. Without any additional purification, all compounds were utilized just as supplied.

Catalyst Preparation

The Ni/MgO catalysts were prepared with different Ni loadings (10%–40% by weight) using the wet impregnation method. To prepare a certain amount of catalyst with 10% Ni loading, 0.496 g of $Ni(NO_3)_2.6H_2O$ was dissolved in deionized water. After that, this solution was combined with commercially available MgO and agitated for three hours at 50°C. The wet catalyst was dried overnight in an oven (Memmert, Germany) at 110 °C.

The dry catalyst was calcined for three hours at 500 °C in a tube furnace (Carbolite Gero, UK) with static air. The calcined catalyst was stored in air-tight glass bottles in a desiccator. Prior to use in the reactor, the catalyst was reduced in the tube furnace under hydrogen flow (50 mL/min) at 500 °C for 3 hours.

Catalyst Characterization

The calcined catalysts were characterized by X-ray diffraction (XRD) using a D8 DISCOVER X-ray diffractometer (Bruker, Germany). Cu–Kα radiation (λ = 0.15418 nm) was installed in the apparatus, and a scintillation detector running at room temperature, 40 kV, and 40 mA was used. The powder samples were scanned at a pace of 1.4 seconds per step, with an increment of 0.04° from 20° to 85° (2θ). The phase was identified by comparing the XRD spectrum with the JCPDS data cards.

A Quantachrome® ASiQwin™ gas adsorption device (Quantachrome Instruments, USA) was used to study nitrogen adsorption at -196 °C. The powder samples were degassed at 250°C for 3 hours under a secondary vacuum before the nitrogen adsorption test at P/Po = 0.3. The samples' surface areas were determined using the BET equation.

A Quantachrome® Autosorb iQ chemisorption analyzer (Quantachrome Instruments, USA) was used to perform the H_2-TPR (temperature-programmed reduction with hydrogen) examination of the catalysts. The catalyst sample (100 mg) was purged in helium flow for one hour prior to the TPR experiment. The TPR study was then performed with a linear heating rate of 10 K/min while hydrogen was flowing from 353 K to 1173 K. A thermal conductivity detector was used to track the amount of hydrogen consumed (TCD).

SEM (scanning electron microscopy) was used to investigate the catalyst shape and particle distribution using an Evo LS10 scanning electron microscope (Zeiss, Germany).

Catalyst Performance Evaluation

A benchtop stainless steel autoclave reactor (Parr 4566, Parr Instruments, USA) was used for the catalyst performance evaluation. The reactor had a capacity of 300 mL and was equipped with temperature and pressure sensors and a mechanical stirrer. Figure 1 displays the layout of the setup for the experiment.

A typical experiment involved adding 1 g of freshly reduced catalyst to the reactor after adding 100 mL of feed solution (10 weight percent glycerol in water). The reactor was sealed and purged with high-purity nitrogen at least five times to get rid of any air within. In the same manner, hydrogen was added in place of nitrogen. Prior to initiating the experiment, the reactor was examined for leaks for two hours after being pressurized with hydrogen to the required pressure of 3–5 MPa. With the Parr 4848 Reactor Controller (Parr Instruments, USA), the temperature (200–240°C) and stirring rate (500 rpm) were automatically adjusted.

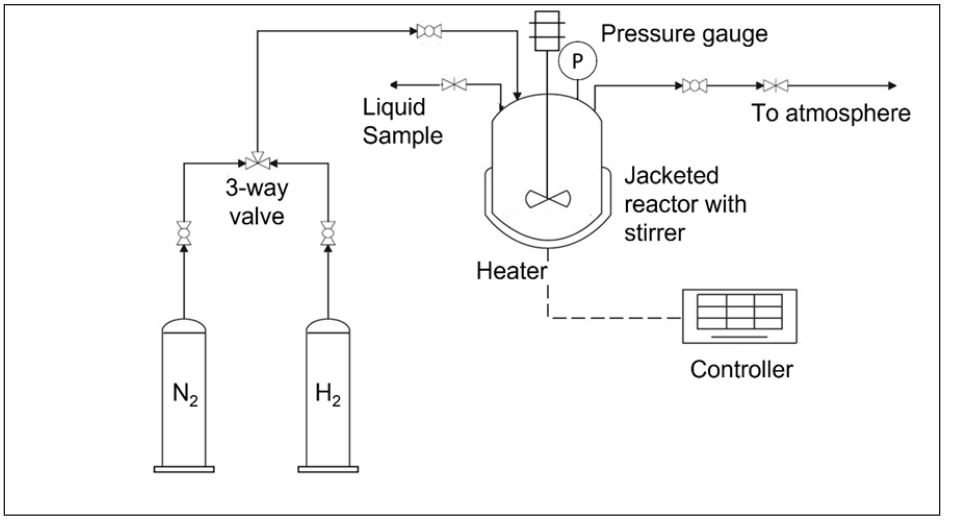

Figure 1. Reactor setup for catalyst evaluation

After the appropriate reaction time had passed (6–25 h), the reactor was quenched by being plunged into an ice bath, and samples of the liquid and gaseous products were collected through the respective sampling ports. The catalyst in the liquid sample was removed by filtration followed by centrifugation at 10,000 rpm for 10 min. All experiments were run in duplicate on different batches of catalysts.

Analysis of Reaction Products

Liquid samples were analyzed by the Shimadzu GC-2014 gas chromatograph (Shimadzu, Japan), which was equipped with an AOC-20i autoinjector, FID, and the HP-Innowax capillary column (30 m × 0.25 mm × 0.25 μm); 1-butanol was used as the internal standard, acetonitrile as the dilution solvent, and nitrogen as the carrier gas. A temperature schedule of injection at 45°C, hold for 4 min, rise to 180°C at 5°C /min and hold for 14 min. Injector temperature: 250°C, detector temperature: 280°C, column flow rate 0.75 mL/min, split ratio 1:50, injection volume 1 μL. Calibration curves were built up for glycerol, 1,2-PDO, 1,3-PDO, 1-propanol, 2-propanol, acetol, ethylene glycol, ethanol and methanol (4 points, R2 > 0.9995). All samples were run twice on the gas chromatograph; the average result is reported here.

The breakdown of glycerol also produces trace amounts of gaseous products. The gaseous samples were examined using a Chromatec Crystal 9000 gas chromatograph (Chromatec, Russia), and the results showed the presence of CO_2, CH_4, and CO_2 in trace levels. However, the composition of the gaseous samples was not quantified.

The overall glycerol conversion, X_{Gly} ,was calculated using Equation 1:

$$X_{Gly}[\%] = \frac{n_{Gly,in} - n_{Gly,out}}{n_{Gly,in}} \times 100 \quad [1]$$

where $n_{Gly,in}$ and $n_{Gly,out}$ represent the total moles of glycerol in the reactor both prior to and following the experiment. The selectivity to any specific product, S_i , was calculated using Equations 2 (Ramesh et al., 2022):

$$S_i[\%] = \frac{\text{carbon moles of product i produced}}{\text{carbon moles of all products}} \times 100 \quad [2]$$

RESULTS AND DISCUSSION

Catalyst Characterization

The crystalline phases of the MgO support and the Ni/MgO catalysts were investigated using X-ray diffraction. To provide an equitable comparison of these data, we have only offset these diffractograms' intensities (Figure 2) rather than rescaling them. Discrete diffraction peaks for the MgO powder at 2θ angles of 36.9°, 42.9°, 62.3°, and 74.7° demonstrate the presence of well-defined MgO crystallites in the support material. Diffraction peaks at 2θ angles of 37.3°, 43.3°, and 79.4° correspond to the crystal planes of NiO(111), NiO(200), and NiO(222) for the Ni/MgO catalysts, respectively. The diffraction peaks corresponding to MgO and NiO are distinctly resolved and can be observed as clearly separated in the XRD pattern. To further emphasize this distinction, a zoomed-in snapshot of the relevant regions of the diffraction pattern has been included in Figure 2. In the case of the Ni/MgO catalysts, these peaks increase in intensity upon increasing the Ni concentration of the catalyst, which again indicates the increased formation of NiO species on the catalytic surface. Interestingly, the diffractograms of Ni/MgO catalysts also present evidence that the catalysts contain a $MgNiO_2$ phase evidenced by diffraction peaks which are somewhat higher at 2θ angles than those of NiO and MgO (Chuanming et al., 2006; Nakayama et al., 1997). Furthermore, the $MgNiO_2$ peaks at roughly 43° and 62° gradually move toward larger 2θ angles as the catalyst's Ni concentration increases. The trends seen in the peak shift are in line with previous research and can be attributed to a greater degree of Mg substitution with Ni in the catalyst structure (Chen et al., 2013). Overall, the presence of the $MgNiO_2$ phase, along with the shifting diffraction peaks, indicates strong metal-support interaction.

Hydrogen consumption analysis of Ni/MgO catalysts was conducted using H_2-TPR studies. The results revealed three distinct reduction peaks observed at around 440 K, 600 K, and 1050 K (Figure 3). According to the literature (Shi et al., 2009; Usman & Daud, 2016), these peaks represent weak, medium-strong, and strong interactions between MgO and NiO. Thus, a low reduction temperature of 440 K indicates that NiO present on the

catalyst surface is weakly bound and, hence, easily reducible. Strong interaction between NiO and the support MgO restricts the reduction of Ni, and the reduction temperature rises.

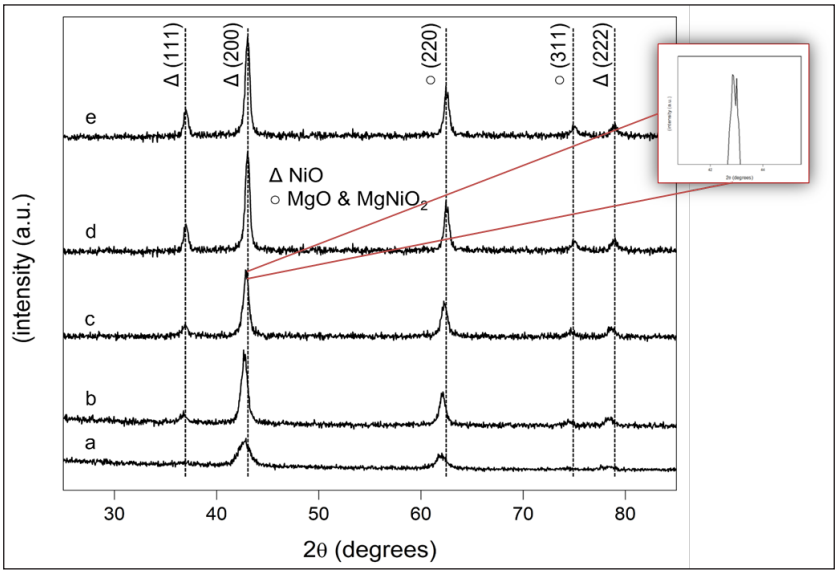

Figure 2. XRD spectra of Ni/MgO catalysts: (a) MgO, (b) 10%Ni/MgO, (c) 20%Ni/MgO, (d) 30%Ni/MgO, (e) 40%Ni/MgO

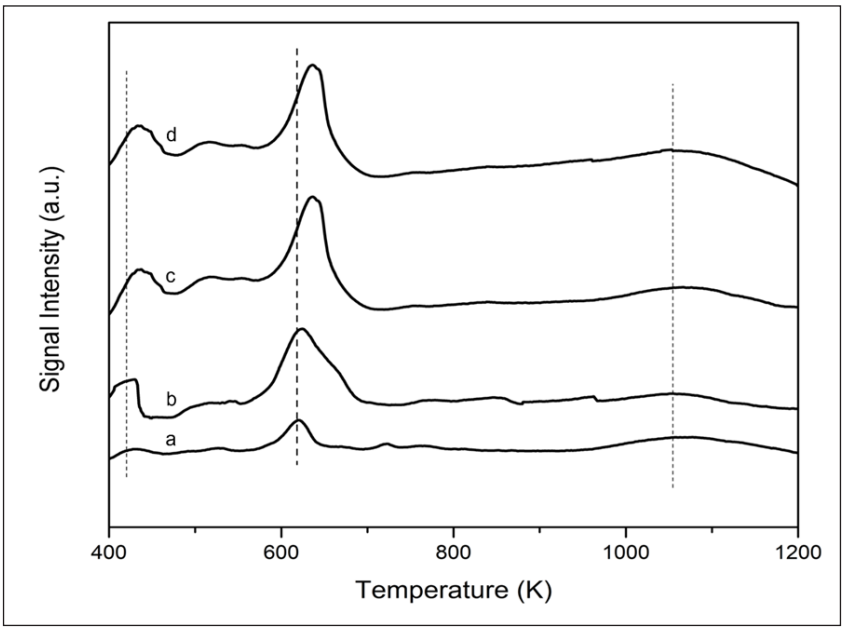

Figure 3. H_2-TPR curves for Ni/MgO catalysts: (a) 10%Ni/MgO, (b) 20%Ni/MgO, (c) 30%Ni/MgO, (d) 40%Ni/MgO

At higher Ni loadings (30%–40%), the H_2-TPR curves show minimal variation around the reduction peaks at 440 K and 600 K. However, increasing nickel loading makes the reduction peak near 1050 K more noticeable. Catalysts with elevated Ni loadings (30%–40%) display reduced hydrogen consumption across all temperatures, further indicating a stronger interaction of Ni and MgO, potentially leading to the formation of $MgNiO_2$ solid solution, as confirmed by the XRD analysis.

SEM-EDX images show that at low Ni loading, Ni distribution on the catalyst support is relatively homogenous (Figure 4). However, as the Ni content is increased, Ni particles have a noticeable agglomeration, which is particularly prominent for the 40%Ni/MgO catalyst (Figure 4d). This is consistent with the XRD analysis and can be explained by the increased formation of the $MgNiO_2$ solid solution at high Ni loading (Echegoyen et al., 2007). Overall, the catalyst with 20% Ni loading appears to have the best surface dispersion of Ni among all synthesized catalysts. Additionally, the EDX analysis for all four catalysts, along with the weight percentages of Ni and Mg prior to the reduction process, is presented in Figure 4. The EDX results demonstrate a clear increase in Ni content as the Ni loading progressively increases.

The results of the BET analysis reflect a similar trend, as presented in Table 1. The surface area and pore volume of the MgO support are comparatively high. However, applying a tiny amount of Ni (10% loading) to the support reduces its pore volume and surface area to about half its original value. This is frequently observed in catalysts that have been prepared by wet impregnation and is explained by the Ni particles blocking the pores of the catalyst. Further additions of Ni loading further reduce the catalyst surface area and pore volume. This agrees with a progressive increase in the dimensions of the Ni particles and an accompanying rise in the pore-blocking effect. This effect is most pronounced for the 40%Ni/MgO catalyst, as expected from the corresponding XRD and SEM analyses.

Table 1
Catalyst surface area and pore volume from BET analysis

Catalyst	**Surface Area [m^2/g]**	**Pore volume* [$\times 10^{-2}$ cm^3/g]**
MgO	172.57	8.54
10%Ni/MgO	78.26	3.92
20%Ni/MgO	71.30	3.31
30%Ni/MgO	56.07	2.79
40%Ni/MgO	29.22	1.46

*The pore volume of the catalysts was calculated using a relative pressure (P/Po) of 0.3

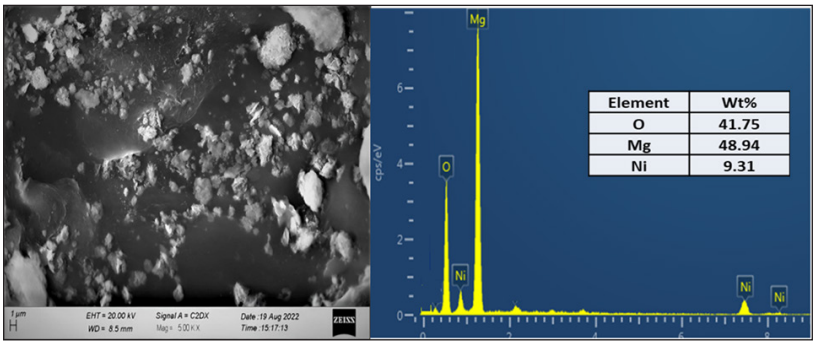

(a)

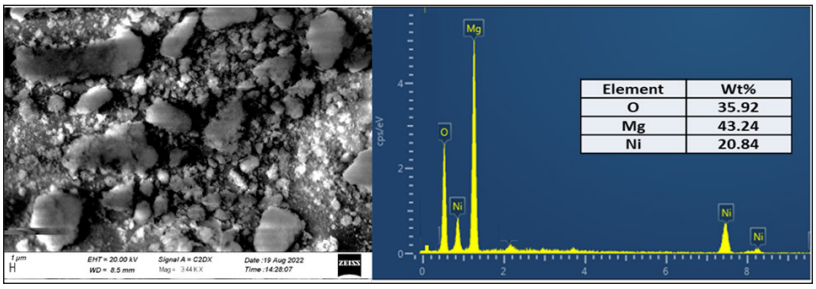

(b)

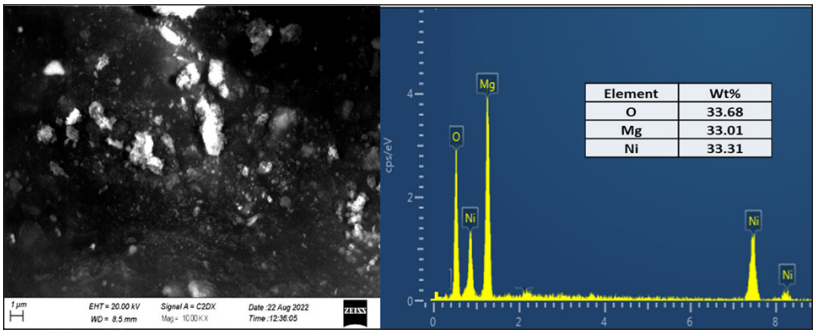

(c)

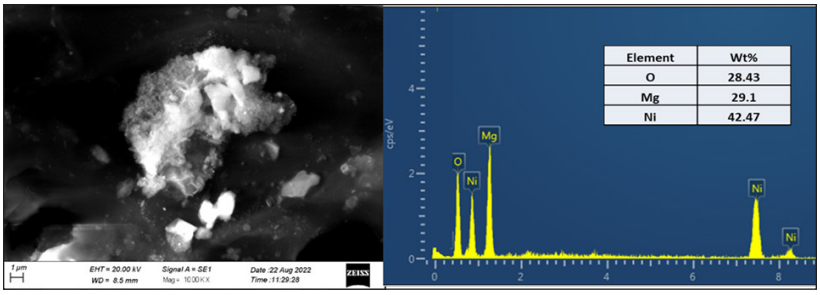

(d)

Figure 4. SEM-EDX images of Ni/MgO catalysts: (a) 10%Ni/MgO, (b) 20%Ni/MgO, (c) 30%Ni/MgO, (d) 40%Ni/MgO Catalyst Performance Evaluation

In the first blank experiment, the hydrogenolysis of glycerol was studied in the absence of a catalyst. The reaction conditions included 10 wt.% glycerol in water, 220°C temperature, 3 MPa hydrogen pressure, and 20 hours reaction time. No conversion of glycerol was observed at the end of the experiment. We conclude that the hydrogenolysis reaction cannot proceed spontaneously under these reaction conditions. In the second blank experiment, the hydrogenolysis was carried out under the same reaction conditions but in the presence of MgO support without any Ni metal added to it. A very low conversion of glycerol (<3%) was obtained, and no 1,2-PDO was detected in the liquid mixture. We conclude from this that MgO alone has little influence on the decrease in the energy activation of glycerol hydrogenolysis.

Significantly higher glycerol conversion was recorded when the glycerol hydrogenolysis was performed in the presence of Ni/MgO catalyst under identical reaction conditions. The liquid product mixture mainly consisted of 1,2-PDO, 2-propanol and unconverted glycerol. In addition, in minor quantities, ethylene glycol, methanol, acetol, 1-propanol, and ethanol were present.

Table 2
Effect of Ni loading on the conversion of glycerol (10 wt.% glycerol solution, 220°C temperature, 3 MPa hydrogen pressure, 20 hours reaction time)

Catalyst	Glycerol Conversion [%]	Selectivity [%][a]				
		1,2-PDO	2-Propanol	Ethylene Glycol	Methanol	Others[b]
Blank	-	-	-	-	-	-
MgO	<3%	-	-	-	-	-
10%Ni/MgO	47.3	80	9	5	5	2
20%Ni/MgO	74.2	76	13	7	3	2
30%Ni/MgO	80.6	67	19	7	5	2
40%Ni/MgO	87.9	65	21	9	4	2

[a]The calculated selectivity has been rounded to the nearest integer
[b]Others include acetol (detected in all experiments, 0.4%–2%), 1-propanol (detected in all experiments, 0.3–0.8%), and ethanol (detected in some experiments, ~0.1%)

Table 2 also shows that while increasing the Ni loading from 10% to 20%, the conversion of glycerol increased significantly from 47% to 74%, whereas the selectivity of 1,2-PDO remained almost the same, with a marginal decrease from 80% to 76%. Further increasing the Ni loading to 40%, the glycerol conversion further increased to 88%, whereas the selectivity of 1,2-PDO decreased gradually to 65%. All of them provided a general trend where the conversion of glycerol was in the order of 10%Ni/MgO < 20%Ni/MgO < 30%Ni/MgO < 40%Ni/MgO, whereas selectivity to 1,2-PDO was in the order of 10%Ni/MgO > 20%Ni/MgO > 30%Ni/MgO > 40%Ni/MgO. While the conversion of glycerol

increases, there is a distinct increase in the production of 2-propanol. This is normal because, under these reaction conditions, 1,2-PDO may further undergo hydrogenolysis into 2-propanol (Wang et al., 2022). Another important observation is the consistent increase in the production of cracking products, ethylene glycol and methanol, at high Ni loading. This is in accordance with earlier research that demonstrated Ni is an effective catalyst for C–C bond breakage (Davda et al., 2005; El Doukkali et al., 2020). The 20%Ni/MgO catalyst generally showed the best balance of glycerol conversion and 1,2-PDO selectivity since it had a high surface area and good Ni dispersion, as evidenced by the catalyst characterization tests.

A comparison of the catalysts created in this investigation with those documented in the literature is shown in Table 3. The present review demonstrates that the Ni/MgO catalysts developed in this work have comparable amounts of glycerol conversion and 1,2-PDO selectivity. Coupled with their low cost and the relative ease of synthesis using well-established techniques, this makes them a suitable candidate for further evaluation and optimization of reaction conditions.

Table 3
Comparison of glycerol conversion and 1,2-PDO selectivity over several Ni-based catalysts tested under batch conditions

Catalyst	**Experimental Conditions T [°C]/P [MPa]/Reaction time [h]/ Feed Conc. [wt.%]**	**Glycerol Conversion [%]**	**1,2-PDO Selectivity [%]**	**Reference**
Ni/C	200°C/1.4 MPa/24 h/80%	39.8	68.6	Dasari et al. (2005)
Ni/SiO_2-Al_2O_3	200°C/1.4 MPa/24 h/80%	45.1	64.5	Dasari et al. (2005)
Ni/HDT	220°C/ 3.4 MPa/24 h/60%	47.8	100	Lopez et al. (2019)
Ni/NaX	200°C/6 MPa/10 h/25%	94.5	72.1	Zhao et al. (2010)
Co/MgO	200°C/2 MPa/9 h/10%	44.8	42.2	Guo et al. (2009)
Ni/MgO	220°C/3 MPa/20 h/10%	74.2	76	This work

Reaction Mechanism

Three different mechanisms have been proposed for glycerol hydrogenolysis over supported metal catalysts. These consist of the direct hydrogenolysis mechanism, the dehydration–hydrogenation mechanism, and the dehydrogenation–dehydration-hydrogenation mechanism (Y. Wang et al., 2015). The product distribution analysis shows that a quantifiable amount of acetol is present in all experiments (Table 2). Glycerol is dehydrated to produce acetol (Figure 5). This process takes place on sites that are either very acidic or basic, such as MgO (Kinage et al., 2010; Stošić et al., 2012; Velasquez et al.,

2014). Acetol is then hydrogenated on metallic Ni sites to produce 1,2-PDO. According to Gandarias et al. (2010), these data align with the dehydration–hydrogenation mechanism. We note here that dehydration of glycerol can involve either the terminal –OH group (resulting in acetol) or the middle –OH group (resulting in 3-hydroxypropionaldehyde). Hydrogenation of 3-hydroxypropionaldehyde produces 1,3-PDO, which was not detected in any experiment. Based on Ni/MgO catalysts, we deduce that the terminal –OH group is important for the early dehydration of glycerol.

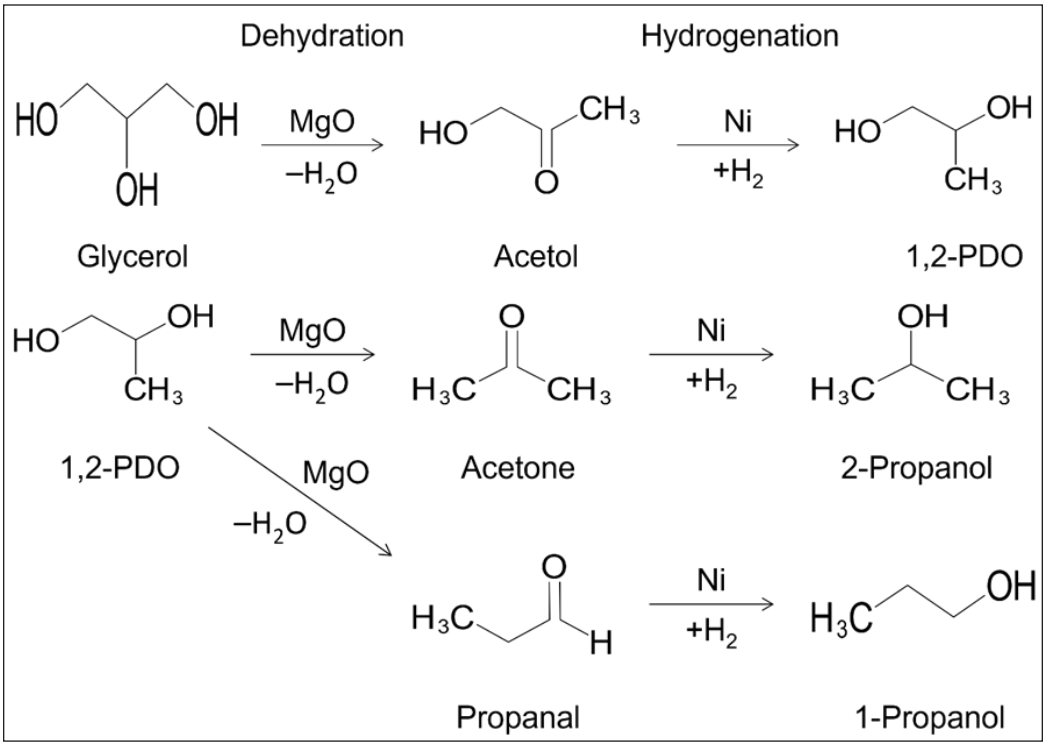

Figure 5. Proposed reaction pathway for the hydrogenolysis of glycerol

On the other hand, the dehydrogenation–dehydration–hydrogenation mechanism goes through glyceraldehyde and pyruvaldehyde intermediates. We note here that no significant peak in any chromatogram was left unquantified. Furthermore, considering the excellent hydrogenation activity of Ni and the hydrogen-rich reaction atmosphere, the initial dehydrogenation of glycerol is highly unlikely to occur, effectively shutting down this reaction pathway.

Because glycerol and 1,2-PDO have similar molecular structures, deep hydrogenolysis is possible under these reaction conditions. Dehydration of 1,2-PDO through the terminal—OH group produces acetone, which is then hydrogenated to produce 2-propanol. On the other hand, dehydration of 1,2-PDO through the mid-chain –OH group forms

propionaldehyde (propanol), which subsequently undergoes hydrogenation to 1-propanol. As shown in Table 2, the selectivity to 2-propanol is always many times higher than that to 1-propanol. We conclude that the dehydration of 1,2-PDO also predominantly proceeds through the terminal –OH group. Further hydrogenolysis of 1- and 2-propanol would produce propane, which was not detected in any experiment.

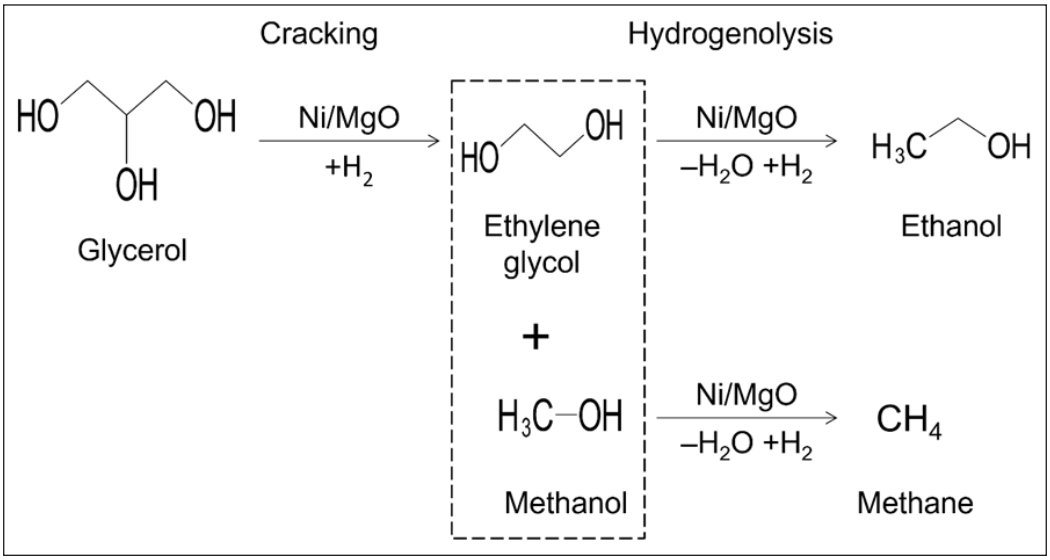

Figure 6. Possible cracking reactions during the hydrogenolysis of glycerol

Cleavage of C–C bonds in glycerol presents another selectivity challenge. Figure 6 illustrates how glycerol splits into a hydrogen-rich environment to create methanol and ethylene glycol. Both these products were present in quantifiable amounts in all experiments. Further hydrogenolysis of ethylene glycol and methanol produces ethanol and methane, respectively. These products were detected only in small quantities.

Likewise, Table 2 demonstrates that when Ni loading increases, the production of byproducts increases. This is observed both in terms of deep hydrogenolysis and cracking pathways, consistent with previous studies (Wolosiak-Hnat et al., 2013). We conclude that under these reaction conditions, glycerol conversion proceeds primarily through hydrogenolysis, with undesired reactions presenting serious selectivity challenges at high Ni loading.

Effect of Reaction Conditions

The 20%Ni/MgO catalyst produced the highest yield of 1,2-PDO through a combination of good glycerol conversion and high selectivity toward 1,2-PDO. It was chosen for additional research to examine the impact of reaction circumstances.

Effect of Temperature

To investigate the effect of temperature on the hydrogenolysis of glycerol, a 20% Ni/MgO catalyst was utilized, and the reaction temperature was changed from 200°C to 240°C. Other reaction conditions were kept fixed, including 10 wt.% glycerol feed, 3 MPa hydrogen pressure, and 20 hours of reaction time. The findings showed that the selectivity of 1,2-PDO and glycerol conversion are both significantly influenced by the reaction temperature (Figure 7). The glycerol conversion rises gradually with increasing reaction temperature, reaching 100% at 240°C from 61% at 200°C. Selectivity for 1,2-PDO has a reverse trend, progressively declining from 82% at 200°C to barely 60% at 240°C. Additionally, there is a noticeable rise in the generation of propanols, with 2-propanol production rising from 9% at 200°C to 24% at 240°C and 1-propanol production rising from 0% at 200°C to 4% at 240°C. From that, we can also infer that higher temperatures increase the glycerol conversion because of an increase in the reaction rate constant since, under such conditions, the hydrogenolysis reaction is not equilibrium-limited.

On the other hand, such excessive hydrogenolysis,2-PDO at elevated temperatures to produce more propanol, causes a decrease in 1,2-PDO. Higher temperatures promote glycerol cracking and reforming over Ni-based catalysts (Mondal & Biswas, 2022), resulting in lower total liquid phase carbon recovery, indicating an increase in the creation of gaseous substances.

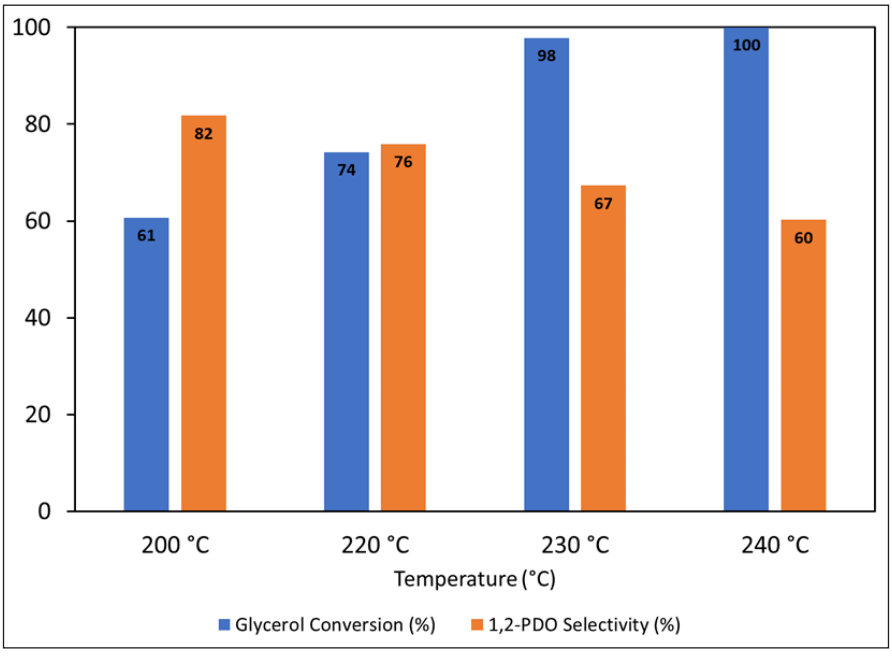

Figure 7. Effect of temperature on the hydrogenolysis of glycerol (20%Ni/MgO catalyst, 10 wt.% glycerol solution, 3.0 MPa hydrogen pressure, 20 hours reaction time)

Effect of Glycerol Concentration

To study the influence of feed concentration, the glycerol concentration of the feed solution varied from 5 weight percent to 30 weight percent in the hydrogenolysis of glycerol over the catalyst of 20%Ni/MgO. The reaction temperature was held constant at 220°C, the hydrogen pressure was kept invariant at 3 MPa, and the reaction time was kept constant at 20 hours. It is evident from the results that the glycerol conversion decreased from 100% in the case of a relatively dilute feed solution of 5 wt% to only 44% in the case of a concentrated feed solution of 30 wt% (Figure 8). This would, therefore, suggest that the concentration of the feed is of particular importance regarding glycerol conversion. This limit in the number of active Ni sites available, even for far larger amounts of glycerol molecules present in the reaction mixture, provides the basis for the observed decrease in conversion at higher glycerol concentrations. Another possible explanation, though not investigated in this study, is the possibility of increased mass transfer resistance around catalyst particles due to increased viscosity of the reaction mixture at higher glycerol concentrations (Cai, Pan et al., 2018; Cai et al., 2016).

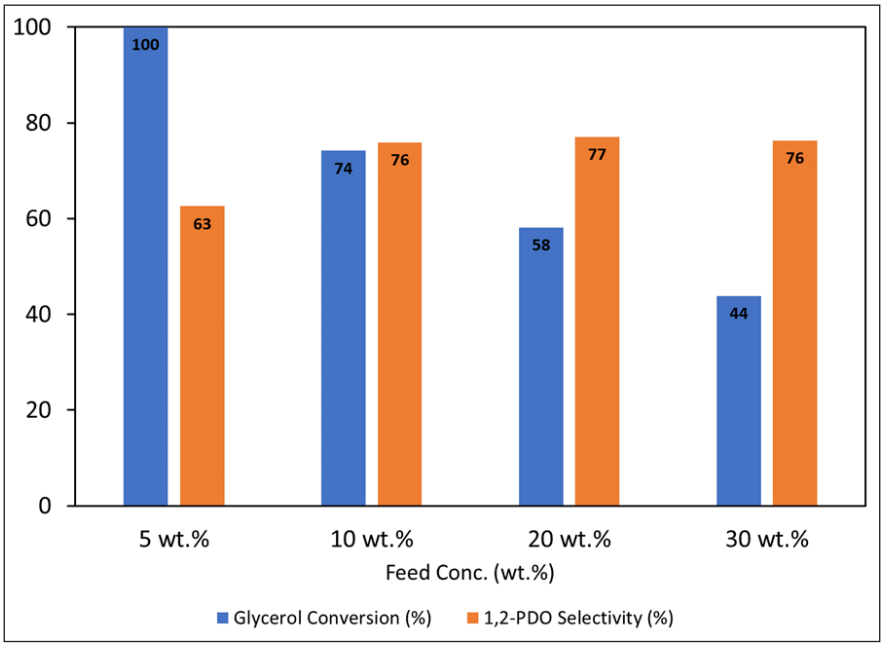

Figure 8. Effect of feed concentration on the hydrogenolysis of glycerol (20%Ni/MgO catalyst, 220°C temperature, 3.0 MPa hydrogen pressure, 20 hours reaction time)

The selectivity towards 1,2-PDO reached as high as 76% in the case of a 10 wt.% feed solution and remained almost constant at this level when the glycerol concentration of the feed solution was increased further to 20 wt.% and 30 wt.%. In these cases, 2-propanol

production also remained almost constant in the range of 10%–12%. This perfectly aligns with the previously reported behavior of Ru and Ni-based catalysts (Alhanash et al., 2008; Yu et al., 2010)—only the feed solution of 5 wt.% showed a considerably lower 1,2-PDO selectivity of 63% and increased production of 2-propanol as high as 23%. From these results, we conclude that beyond the complete conversion of glycerol, the reaction of hydrogenolysis of 1,2-PDO continues and, as such, is responsible for the decrease of 1,2-PDO selectivity observed towards the end of the test.

Effect of Reaction Time

Using a 20%Ni/MgO catalyst, reaction periods ranging from 6 to 25 hours were employed to investigate the impact of reaction length on glycerol hydrogenolysis. Other reaction parameters that were held constant were the feeding of 10% glycerol, the reaction temperature of 220°C, and the hydrogen pressure of 3 MPa. The results show that the glycerol conversion steadily increases for longer reaction times, rising from 64% after 6 hours to 84% after 25 hours (Figure 9). The 1,2-PDO selectivity does, however, significantly decrease with extended reaction periods, indicating that longer reaction times cause deeper hydrogenolysis, which ultimately results in the undesirable destruction of 1,2-PDO. Overall, a reaction time of 12–20 hours is reasonable under these reaction conditions.

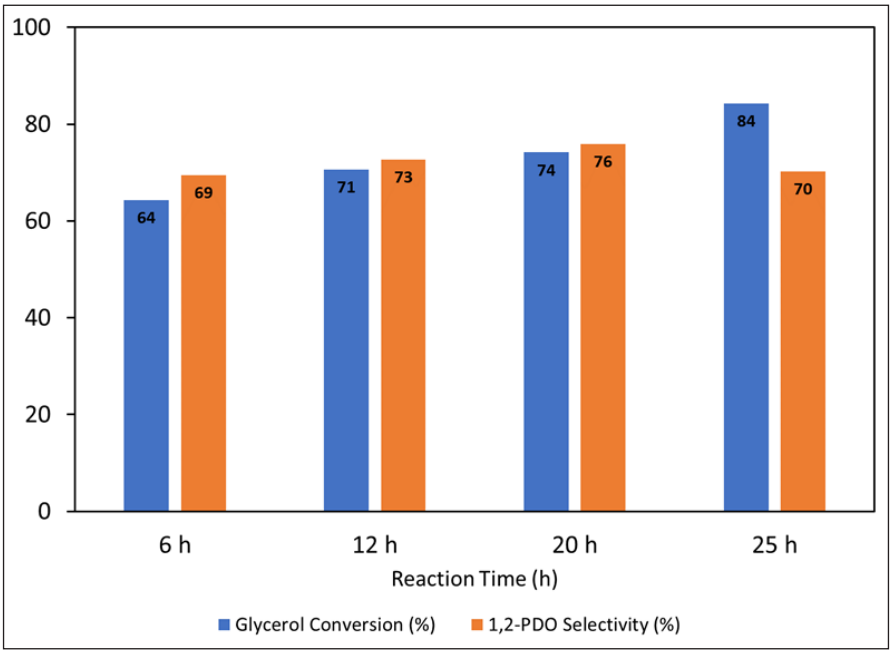

Figure 9. Effect of reaction time on the hydrogenolysis of glycerol (20%Ni/MgO catalyst, 10 wt.% glycerol solution, 220°C temperature, 3.0 MPa hydrogen pressure)

Effect of Pressure

The total hydrogen pressure was changed from 3 MPa to 5 MPa to investigate the effect of pressure on the hydrogenolysis of glycerol using the 20%Ni/MgO catalyst. A 10-weight percent glycerol feed, a reaction temperature of 220°C, and a 20-hour reaction duration were further predetermined reaction parameters. According to the data (Figure 10), glycerol conversion increased steadily at greater pressures. At 3 MPa hydrogen pressure, the acetol concentration in the final mixture drops significantly to less than 0.4%, but the 1,2-PDO selectivity stays relatively stable at 76%–78%. Higher gas phase hydrogen pressure causes hydrogen to dissolve more readily in the liquid reaction mixture. This increased availability of hydrogen near the catalyst facilitates rapid hydrogenation of acetol and, hence, a slight increase in the production of 1,2-PDO over acetol.

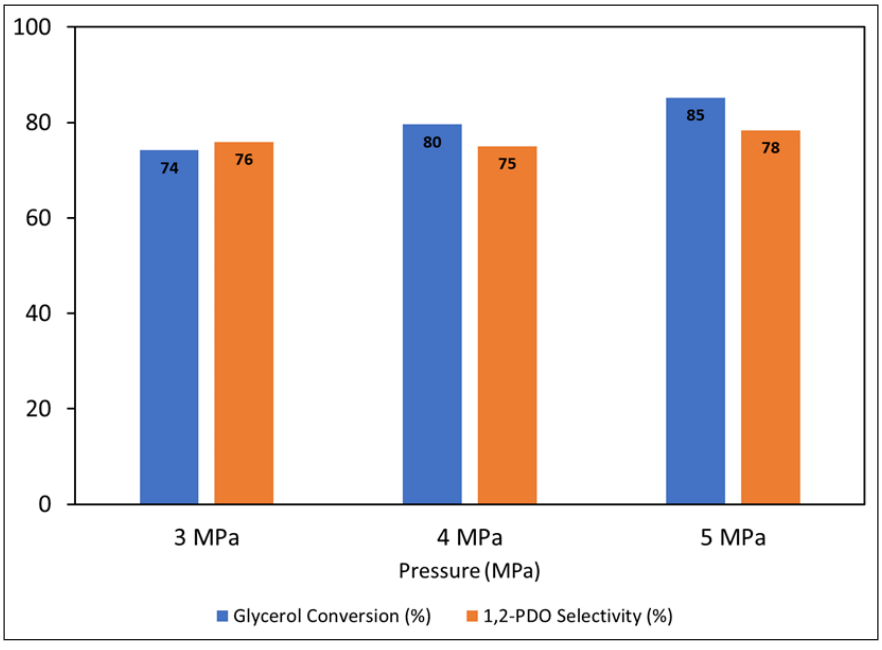

Figure 10. Effect of pressure on the hydrogenolysis of glycerol (20%Ni/MgO catalyst, 10 wt.% glycerol solution, 220°C temperature, 20 hours reaction time)

We highlight that in terms of cost-effectiveness, the aim should be to achieve the desired level of glycerol hydrogenolysis at lower operating pressures to reduce equipment costs. Considering the relatively small gain in glycerol conversion by increasing the total pressure but a potentially significant increase in equipment cost, a hydrogen pressure of 3–4 MPa is recommended.

CONCLUSION

The current work concentrated on synthesizing and characterizing Ni/MgO catalysts made with different Ni loadings using the wet impregnation approach. Under specific reaction circumstances (20 hours of reaction time, 220°C temperature, 3 MPa hydrogen pressure, and 10% weight percent glycerol solution in water), the catalyst with 20% Ni loading (20%Ni/MgO) demonstrated a strong combination of activity and selectivity. This catalyst showed a 76% selectivity toward 1,2-PDO and a 74% glycerol conversion. The catalyst's remarkable performance can be attributed to its small particle size, optimal metal-support interaction, and good Ni concentration and dispersion. It was discovered that the main chemical pathway involved the hydrogenation of acetol to 1,2-PDO after glycerol was dehydrated to acetol. Side reactions, including C-C bond breakage and extra 1,2-PDO hydrogenolysis, were more prevalent when reaction times were extended and Ni loadings were high. Several reaction conditions were subsequently analyzed, and the results indicated that they significantly affected the glycerol conversion and the selectivity of 1,2-PDO. It was discovered that the ideal values for temperature, pressure, feed concentration, and reaction time were 220°C, 3 MPa, 10 weight percent glycerol concentration, and 20 hours, respectively. Due to these conditions, a reasonable trade-off between 1,2-PDO selectivity and glycerol conversion could be reached, highlighting the importance of carefully controlling the reaction conditions to maximize the desired product's yield.

Overall, this work's results advance our knowledge of the hydrogenolysis process using Ni/MgO catalysts. The developed catalyst and optimized reaction conditions provide valuable insights for future research and potential industrial applications in glycerol conversion processes.

ACKNOWLEDGEMENTS

The Higher Education Commission of Pakistan provided financial support (grant number NRPU-9360) to the authors, which they sincerely acknowledge. M.S. also thanks the Higher Education Commission of Pakistan for funding assistance the Indigenous PhD Fellowships for 5000 Scholars (Phase II) program provides.

REFERENCES

Alhanash, A., Kozhevnikova, E. F., & Kozhevnikov, I. V. (2008). Hydrogenolysis of glycerol to propanediol over Ru: Polyoxometalate bifunctional catalyst. *Catalysis Letters*, *120*, 307–311. https://doi.org/10.1007/s10562-007-9286-3

Azri, N., Irmawati, R., Nda-Umar, U. I., Saiman, M. I., & Taufiq-Yap, Y. H. (2021). Promotional effect of transition metals (Cu, Ni, Co, Fe, Zn)–supported on dolomite for hydrogenolysis of glycerol into 1,2-propanediol. *Arabian Journal of Chemistry*, *14*(4), Article 103047. https://doi.org/10.1016/j.arabjc.2021.103047

Bagheri, S., Julkapli, N. M., & Yehye, W. A. (2015). Catalytic conversion of biodiesel derived raw glycerol to value added products. *Renewable and Sustainable Energy Reviews*, *41*, 113–127. https://doi.org/10.1016/j.rser.2014.08.031

Balaraju, M., Jagadeeswaraiah, K., Prasad, P. S. S., & Lingaiah, N. (2012). Catalytic hydrogenolysis of biodiesel derived glycerol to 1,2-propanediol over Cu-MgO catalysts. *Catalysis Science and Technology*, *2*, 1967–1976. https://doi.org/10.1039/C2CY20059G

Cai, F., Pan, D., Ibrahim, J. J., Zhang, J., & Xiao, G. (2018). Hydrogenolysis of glycerol over supported bimetallic Ni/Cu catalysts with and without external hydrogen addition in a fixed-bed flow reactor. *Applied Catalysis A: General*, *564*, 172–182. https://doi.org/10.1016/j.apcata.2018.07.029

Cai, F., Song, X., Wu, Y., Zhang, J., & Xiao, G. (2018). Selective hydrogenolysis of glycerol over acid-modified Co-Al catalysts in a fixed-bed flow reactor. *ACS Sustainable Chemistry and Engineering, 6*(1), 110–118. https://doi.org/10.1021/acssuschemeng.7b01233

Cai, F., Zhu, W., & Xiao, G. (2016). Promoting effect of zirconium oxide on Cu-Al_2O_3 catalyst for the hydrogenolysis of glycerol to 1,2-propanediol. *Catalysis Science and Technology*, *6*, 4889–4900. https://doi.org/10.1039/C6CY00085A

Checa, M., Auneau, F., Hidalgo-Carrillo, J., Marinas, A., Marinas, J. M., Pinel, C., & Urbano, F. J. (2012). Catalytic transformation of glycerol on several metal systems supported on ZnO. *Catalysis Today, 196*(1), 91–100. https://doi.org/10.1016/j.cattod.2012.02.036

Chen, X., Wang, X., Yao, S., & Mu, X. (2013). Hydrogenolysis of biomass-derived sorbitol to glycols and glycerol over Ni-MgO catalysts. *Catalysis Communications*, *39*, 86–89. https://doi.org/10.1016/j.catcom.2013.05.012

Chuanming, L., Donghua, C., Wanjun, T., & Yuhua, P. (2006). Synthesis of $MgNi_2O_3$ and kinetics of thermal decomposition of the oxalate precursor. *Journal of Analytical and Applied Pyrolysis*, *75*(2), 240–244. https://doi.org/10.1016/j.jaap.2005.06.007

Davda, R. R., Shabaker, J. W., Huber, G. W., Cortright, R. D., & Dumesic, J. A. (2005). A review of catalytic issues and process conditions for renewable hydrogen and alkanes by aqueous-phase reforming of oxygenated hydrocarbons over supported metal catalysts. *Applied Catalysis B: Environmental, 56*(1-2), 171–186. https://doi.org/10.1016/j.apcatb.2004.04.027

Dasari, M. A., Kiatsimkul, P. P., Sutterlin, W. R., & Suppes, G. J. (2005). Low-pressure hydrogenolysis of glycerol to propylene glycol. *Applied Catalysis A: General*, *281*, 225–231. https://doi.org/10.1016/j.apcata.2004.11.033

Dolsiririttigul, N., Numpilai, T., Wattanakit, C., Seubsai, A., Faungnawakij, K., Cheng, C. K., Vo, D. V. N., Nijpanich, S., Chanlek, N., & Witoon, T. (2023). Structure-activity relationships of Pt-WOx/Al_2O_3 prepared with different W contents and pretreatment conditions for glycerol conversion to 1,3-propanediol. *Topics in Catalysis*, *66*(1–4), 205–222. https://doi.org/10.1007/S11244-022-01753-9/METRICS

Echegoyen, Y., Suelves, I., Lázaro, M. J., Sanjuán, M. L., & Moliner, R. (2007). Thermo catalytic decomposition of methane over Ni-Mg and Ni-Cu-Mg catalysts. Effect of catalyst preparation method. *Applied Catalysis A: General*, *333*, 229–237. https://doi.org/10.1016/j.apcata.2007.09.012

El Doukkali, M., Iriondo, A., & Gandarias, I. (2020). Enhanced catalytic upgrading of glycerol into high value-added H2 and propanediols: Recent developments and future perspectives. *Molecular Catalysis*, *490*, Article 110928. https://doi.org/10.1016/j.mcat.2020.110928

Gandarias, I., Arias, P. L., Requies, J., Güemez, M. B., & Fierro, J. L. G. (2010). Hydrogenolysis of glycerol to propanediols over a Pt/ASA catalyst: The role of acid and metal sites on product selectivity and the reaction mechanism. *Applied Catalysis B: Environmental*, *97*(1–2), 248–256. https://doi.org/10.1016/j.apcatb.2010.04.008

Gonzalez-Garay, A., Gonzalez-Miquel, M., & Guillen-Gosalbez, G. (2017). High-value propylene glycol from low-value biodiesel glycerol: A techno-economic and environmental assessment under uncertainty. *ACS Sustainable Chemistry and Engineering*, *5*, 5723–5732. https://doi.org/10.1021/acssuschemeng.7b00286

Guo, X., Li, Y., Shi, R., Liu, Q., Zhan, E., & Shen, W. (2009). Co/MgO catalysts for hydrogenolysis of glycerol to 1, 2-propanediol. *Applied Catalysis A: General*, *371*, 108–113. https://doi.org/10.1016/j.apcata.2009.09.037

Kinage, A. K., Upare, P. P., Kasinathan, P., Hwang, Y. K., & Chang, J. S. (2010). Selective conversion of glycerol to acetol over sodium-doped metal oxide catalysts. *Catalysis Communications*, *11*(7), 620–623. https://doi.org/10.1016/j.catcom.2010.01.008

Kumar, P., Shah, A. K., Lee, J. H., Park, Y. H., & Štangar, U. L. (2020). Selective hydrogenolysis of glycerol over bifunctional copper-magnesium-supported catalysts for propanediol synthesis. *Industrial and Engineering Chemistry Research*, *59*, 6506–6516. https://doi.org/10.1021/acs.iecr.9b06978

López, A., Aragón, J. A., Hernández-Cortez, J. G., Mosqueira, M. L., & Martínez-Palou, R. (2019). Study of hydrotalcite-supported transition metals as catalysts for crude glycerol hydrogenolysis. *Molecular Catalysis*, *468*, 9–18. https://doi.org/10.1016/j.mcat.2019.02.008

Menchavez, R. N., Morra, M. J., & He, B. B. (2017). Glycerol hydrogenolysis using a Ni/Ce-Mg catalyst for improved ethanol and 1,2-propanediol selectivities. *Canadian Journal of Chemical Engineering*, *95*(7), 1332–1339. https://doi.org/10.1002/cjce.22779

Mondal, S., & Biswas, P. (2022). Conversion of bio-glycerol to propylene glycol over basic oxides (MgO, La_2O_3, MgO-La_2O_3, CaO, and BaO_2) supported Cu–Zn bimetallic catalyst: A reaction kinetic study. *Environmental Technology & Innovation*, *27*, Article 102367. https://doi.org/10.1016/j.eti.2022.102367

Nakagawa, Y., & Tomishige, K. (2011). Heterogeneous catalysis of the glycerol hydrogenolysis. *Catalysis Science & Technology, 1*(2), 179-190. https://doi.org/10.1039/C0CY00054J

Numpilai, T., Cheng, C. K., Seubsai, A., Faungnawakij, K., Limtrakul, J., & Witoon, T. (2021). Sustainable utilization of waste glycerol for 1,3-propanediol production over Pt/WOx/Al_2O_3 catalysts: Effects of catalyst pore sizes and optimization of synthesis conditions. *Environmental Pollution*, *272*, Article 116029. https://doi.org/10.1016/J.ENVPOL.2020.116029

Nakayama, T., Ichikuni, N., Sato, S., & Nozaki, F. (1997). Ni/Mgo catalyst prepared using citric acid for hydrogenation of carbon dioxide. *Applied Catalysis A: General*, *158*(1–2), 185–199. https://doi.org/10.1016/S0926-860X(96)00399-7

Quispe, C. A. G., Coronado, C. J. R., & Carvalho, J. A. (2013). Glycerol: Production, consumption, prices, characterization and new trends in combustion. *Renewable and Sustainable Energy Reviews, 27*, 475–493. https://doi.org/10.1016/j.rser.2013.06.017

Ramesh, A., Ali, B. M., Manigandan, R., Da, C. T., & Nguyen-Le, M. T. (2022). Hydrogenolysis of glycerol to 1, 2-propanediol on MgO/Ni_3C catalysts fabricated by a solid-state thermal synthesis. *Molecular Catalysis*, *525*, Article 112358. https://doi.org/10.1016/j.mcat.2022.112358

Rivas, M. E., Hori, C. E., Fierro, J. L. G., Goldwasser, M. R., & Griboval-Constant, A. (2008). H_2 production from CH_4 decomposition: Regeneration capability and performance of nickel and rhodium oxide catalysts. *Journal of Power Sources*, *184*, 265–275. https://doi.org/10.1016/j.jpowsour.2008.06.002

Rogers, J. L., Mangarella, M. C., D'Amico, A. D., Gallagher, J. R., Dutzer, M. R., Stavitski, E., Miller, J. T., & Sievers, C. (2016). Differences in the nature of active sites for methane dry reforming and methane steam reforming over nickel aluminate catalysts. *ACS Catalysis*, *6*, 5873–5886. https://doi.org/10.1021/acscatal.6b01133

Ross, J. R. H., Steel, M. C. F., & Zeini-Isfahani, A. (1978). Evidence for the participation of surface nickel aluminate sites in the steam reforming of methane over nickel/alumina catalysts. *Journal of Catalysis*, *52*, 280–290. https://doi.org/10.1016/0021-9517(78)90142-2

Raju, N., Rekha, V., Abhishek, B., Kumar, P. M., Sumana, C., & Lingaiah, N. (2020). Studies on continuous selective hydrogenolysis of glycerol over supported Cu-Co bimetallic catalysts. *New Journal of Chemistry*, *44*(7), 3122–3128. https://doi.org/10.1039/c9nj04945b

Rekha, V., Raju, N., Sumana, C., & Lingaiah, N. (2017). Continuous hydrogenolysis of glycerol to 1,2-Propanediol over Bi-metallic Ni–Ag supported on $_{\gamma}$-Al_2O_3 catalysts. *Catalysis Letters*, *147*(6), 1441–1452. https://doi.org/10.1007/s10562-017-2052-2

Salgado, A. L. P., Araújo, F. C., Soares, A. V. H., Xing, Y., & Passos, F. B. (2021). Glycerol hydrogenolysis over Ru-Cu bimetallic catalysts supported on modified zirconias. *Applied Catalysis A: General*, *626*, Article 118359. https://doi.org/10.1016/j.apcata.2021.118359

Stošić, D., Bennici, S., Sirotin, S., Calais, C., Couturier, J. L., Dubois, J. L., Travert, A., & Auroux, A. (2012). Glycerol dehydration over calcium phosphate catalysts: Effect of acidic-basic features on catalytic performance. *Applied Catalysis A: General*, *447–448*, 124–134. https://doi.org/10.1016/j.apcata.2012.09.029

Seretis, A., & Tsiakaras, P. (2016). Hydrogenolysis of glycerol to propylene glycol by in situ produced hydrogen from aqueous phase reforming of glycerol over SiO_2-Al_2O_3 supported nickel catalyst. *Fuel Processing Technology*, *142*, 135–146. https://doi.org/10.1016/j.fuproc.2015.10.013

Shi, Q., Liu, C., & Chen, W. (2009). Hydrogen production from steam reforming of ethanol over Ni/MgO-CeO_2 catalyst at low temperature. *Journal of Rare Earths*, *27*, 948–954. http://dx.doi.org/10.1016/S1002-0721(08)60368-3

Sun, D., Yamada, Y., Sato, S., & Ueda, W. (2016). Glycerol hydrogenolysis into useful C_3 chemicals. *Applied Catalysis B: Environmental*, *193*, 75–92. https://doi.org/10.1016/j.apcatb.2016.04.013

Tendam, J., & Hanefeld, U. (2011). Renewable chemicals: Dehydroxylation of glycerol and polyols. *ChemSusChem*, *4*, 1017–1034. https://doi.org/10.1002/cssc.201100162

Usman, M., & Daud, W. M. A. W. (2016). An investigation on the influence of catalyst composition, calcination and reduction temperatures on Ni/MgO catalyst for dry reforming of methane. *RSC Advances*, *6*, 91603–91616. https://doi.org/10.1039/C6RA15256B

Vasiliadou, E. S., & Lemonidou, A. A. (2015). Glycerol transformation to value added C_3 diols: Reaction mechanism, kinetic, and engineering aspects. *Wiley Interdisciplinary Reviews: Energy and Environment*, *4*, 486–520. https://doi.org/10.1002/wene.159

van Ryneveld, E., Mahomed, A. S., van Heerden, P. S., Green, M. J., & Friedrich, H. B. (2011). A catalytic route to lower alcohols from glycerol using Ni-supported catalysts. *Green Chemistry*, *13*(7), 1819–1827. https://doi.org/10.1039/c0gc00839g

Velasquez, M., Santamaria, A., & Batiot-Dupeyrat, C. (2014). Selective conversion of glycerol to hydroxyacetone in gas phase over La_2CuO_4 catalyst. *Applied Catalysis B: Environmental*, *160–161*(1), 606–613. https://doi.org/10.1016/j.apcatb.2014.06.006

Wang, S., Yin, K., Zhang, Y., & Liu, H. (2013). Glycerol hydrogenolysis to propylene glycol and ethylene glycol on zirconia supported noble metal catalysts. *ACS Catalysis*, *3*(9), 2112–2121. https://doi.org/10.1021/cs400486z

Wang, S., & Liu, H. (2014). Selective hydrogenolysis of glycerol to propylene glycol on hydroxycarbonate-derived Cu-ZnO-Al_2O_3 catalysts. *Cuihua Xuebao/Chinese Journal of Catalysis*, *35*(5), 631–643. https://doi.org/10.1016/s1872-2067(14)60094-2

Wang, X., Liu, X., Xu, Y., Peng, G., Cao, Q., & Mu, X. (2015). Sorbitol hydrogenolysis to glycerol and glycols over M-MgO (M = Ni, Co, Cu) nanocomposite: A comparative study of active metals. *Cuihua Xuebao/Chinese Journal of Catalysis*, *36*(9), 1614–1622. https://doi.org/10.1016/S1872-2067(15)60928-7

Wang, Y., Zhou, J., & Guo, X. (2015). Catalytic hydrogenolysis of glycerol to propanediols: A review. *RSC Advances* (5, 91, 74611–74628). https://doi.org/10.1039/c5ra11957j

Wang, Y., Xiao, Y., & Xiao, G. (2019). Sustainable value-added C3 chemicals from glycerol transformations: A mini review for heterogeneous catalytic processes. *Chinese Journal of Chemical Engineering*, *27*(7), 1536–1542. https://doi.org/10.1016/j.cjche.2019.03.001

Wu, K., Dou, B., Zhang, H., Liu, D., Chen, H., & Xu, Y. (2021). Effect of impurities of CH_3OH, CH_3COOH, and KOH on aqueous phase reforming of glycerol over mesoporous Ni–Cu/CeO_2 catalyst. *Journal of the Energy Institute*, *99*, 198–208. https://doi.org/10.1016/j.joei.2021.09.009

Wang, J., Wang, M., Li, X., Gu, X., Kong, P., Wang, R., Ke, X., Yu, G., & Zheng, Z. (2022). Bidentate ligand modification strategy on supported Ni nanoparticles for photocatalytic selective hydrogenation of alkynes. *Applied Catalysis B: Environmental*, *313*, Article 121449. https://doi.org/10.1016/j.apcatb.2022.121449

Wolosiak-Hnat, A., Milchert, E., & Grzmil, B. (2013). Influence of Parameters on Glycerol Hydrogenolysis over a Cu/Al_2O_3 Catalyst. *Chemical Engineering & Technology*, *36*, 411–418. https://doi.org/10.1002/ceat.201200549

Xia, S., Nie, R., Lu, X., Wang, L., Chen, P., & Hou, Z. (2012). Hydrogenolysis of glycerol over $Cu_{0.4}/Zn_{5.6}$-x$MgxAl_2O_{8.6}$ catalysts: The role of basicity and hydrogen spillover. *Journal of Catalysis*, *296*, 1–11. https://doi.org/10.1016/j.jcat.2012.08.007

Yu, W., Zhao, J., Ma, H., Miao, H., Song, Q., & Xu, J. (2010). Aqueous hydrogenolysis of glycerol over Ni-Ce/AC catalyst: Promoting effect of Ce on catalytic performance. *Applied Catalysis A: General*, *383*, 73–78. https://doi.org/10.1016/j.apcata.2010.05.023

Zhou, J., Guo, L., Guo, X., Mao, J., & Zhang, S. (2010). Selective hydrogenolysis of glycerol to propanediols on supported Cu-containing bimetallic catalysts. *Green Chemistry*, *12*(10), 1835–1843. https://doi.org/10.1039/c0gc00058b

Zhao, J., Yu, W., Chen, C., Miao, H., Ma, H., & Xu, J. (2010). Ni/NaX: A bifunctional efficient catalyst for selective hydrogenolysis of glycerol. *Catalysis Letters*, *134*, 184–189. https://doi.org/10.1007/s10562-009-0208-4